Since January 2020 Elsevier has created a COVID-19 resource centre with free information in English and Mandarin on the novel coronavirus COVID-19. The COVID-19 resource centre is hosted on Elsevier Connect, the company's public news and information website.

Results in Physics 23 (2021) 103976

Contents lists available at ScienceDirect

Results in Physics

journal homepage: www.elsevier.com/locate/rinp

Investigation of the dynamics of COVID-19 with a fractional mathematical model: A comparative study with actual data

Ismail Gad Ameen [a], Hegagi Mohamed Ali [b], M.R. Alharthi [c], Abdel-Haleem Abdel-Aty [d,e,*], Hillal M. Elshehabey [a,f]

[a] Mathematics Department, Faculty of Science, South Valley University, Qena 83523, Egypt
[b] Department of Mathematics, Faculty of Science, Aswan University, Aswan 81528, Egypt
[c] Department of Mathematics and Statistics, College of Science, Taif University, PO Box 11099, Taif 21944, Saudi Arabia
[d] Department of Physics, College of Sciences, University of Bisha, PO Box 344, Bisha 61922, Saudi Arabia
[e] Physics Department, Faculty of Science, Al-Azhar University, Assiut 71524, Egypt
[f] Instituto Superior Técnico, Universidade de Lisboa, Av. Rovisco Pais 1, 1049-001 Lisboa, Portugal

ARTICLE INFO

Keywords:
Novel coronavirus
Mathematical model
Caputo fractional derivative
Stability
Real data
Numerical simulation

ABSTRACT

One of the greatest challenges facing the humankind nowadays is to confront that emerging virus, which is the Coronavirus (COVID-19), and therefore all organizations have to unite in order to tackle that the transmission risk of this virus. From this standpoint, the scientific researchers have to find good mathematical models that do describe the transmission of such virus and contribute to reducing it in one way or another, where the study of COVID-19 transmission dynamics by mathematical models is very important for analyzing and controlling this disease propagation. Thus, in the current work, we present a new fractional-order mathematical model that describes the dynamics of COVID-19. In the proposed model, the total population is divided into eight classes, in addition to three compartments used to estimate the parameters and initial values. The effective reproduction number (R_0) is derived by next generation matrix (NGM) method and all possible equilibrium points and their stability are investigated in details. We used the reported data (from January 23, 2020, to November 21, 2020) from the National Health Commission (NHC) of China to estimate the parameters and initial conditions (ICs) which suggested for our model. Simulation outcomes demonstrate that the fractional order model (FOM) represents behaviors that follow the real data more accurately than the integer-order model. The current work enhances the recent reported results of Zu et al. published in THE LANCET (doi:10.2139/ssrn.3539669).

1. Introduction

According to what was published in the World Health Organization (WHO) [1], Coronavirus disease (COVID-19) is a newly discovered infectious disease and is a new strain that has not been previously specified in humans. The COVID-19 virus transmitted through closed contact and droplets of saliva or discharge from the nose when an infected person coughs or sneezes at close range. The symptoms of this disease appear in the form of coughing, sore throat, fever, headache, breathing difficulties, fatigue and diarrhea [2–4]. In critical cases, the infected patient has severe pneumonia which leads to death. As a result, the elderly and those with a sick history like diabetes, cardiovascular disease, hypertension, cancer and chronic respiratory disease are more likely to reach critical cases. Till now there are no specific treatments or clear vaccines for COVID-19. However, there are many ongoing clinical trials evaluating potential treatments.

The outbreak of COVID-19 started since 31 December 2019, as the Health Committee of Wuhan Province in China received 27 cases of viral pneumonia, including 7 critical cases. After that, the outbreak of this disease started in different parts of China and different countries such as the United States of America, Singapore, Thailand, South Korea, Mexico and some regions in Europe, where the WHO monitored on 23 January 2020, more than 571 confirmed cases with 17 deaths in China and various countries. As of 6 February 2020, around 28276 cases, of which 3863 are in critical condition, and 565 deaths had been reported. For that, COVID-19 has received considerable global attention and the WHO

* Corresponding author at: Department of Physics, College of Sciences, University of Bisha, PO Box 344, Bisha 61922, Saudi Arabia.
E-mail addresses: ismailgad@svu.edu.eg (I.G. Ameen), hegagi_math@aswu.edu.eg (H.M. Ali), muteb@tu.edu.as (M.R. Alharthi), amabdelaty@ub.edu.sa (A.-H. Abdel-Aty), hilal.hilal@sci.svu.edu.eg (H.M. Elshehabey).

https://doi.org/10.1016/j.rinp.2021.103976
Received 11 January 2021; Received in revised form 7 February 2021; Accepted 8 February 2021
Available online 19 February 2021

released a wide range of interim guidance for all countries on how they can get prepared for coping with this emergency. For more information on the precautionary measures and protocols used to confront this global epidemic, we recommend viewing the following references [5–9]. The fast track in which a virus has spread and the rapid growth in the number of infected cases has led to a global alert for governments, local health organizations and the WHO to take action to control this disease. Within these procedures, a public awareness campaign is being carried out using TV stations, posters and newspapers. Sterilize most public and vital places by spraying with sterile materials. In addition to quarantining people who have direct or indirect contact with infected cases of this virus, either by quarantined in their homes or in quarantined hospitals and strict monitoring of migrants and so on.

One of the important efforts to face COVID-19 is to found a well-mathematical model. Certainly, mathematical models for infectious disease can help forecast the probable path of an epidemic, and detect the most promising and realistic strategies for containing it [10–14]. Moreover, mathematical models can simulate the impacts of diseases by different ways such as how the disease influences the interactions between cells in a single patient (within–host models), how it spreads across several geographically separated populations (metapopulation models) and how it spreads within and between individuals, such as those used to predict the COVID-19 outbreak. There are a few research efforts done to construct mathematical models to study COVID-19 in the form of a system of ordinary differential equations (ODEs), which relied on estimating the initial values and parameters of the model on the data reported by global and national public health (see, e.g. [7,15–22] and some references therein). Since several decades ago, a new branch of mathematics called fractional calculus (FC) appeared which represents a generalization of classical integer order for differentiation and integration. Recently, FC attracted much attention of researchers and became an active research field and by using it, many promising ideas were modeled and proposed in various scientific fields [23–31].

There are several different kinds of definitions for fractional differential operators (FDOs) in the literature such as Caputo, Riemann–Liouville, Jumarie, Hadamard, Gröunwald-Letnikov, Atangana-Baleanu and others (see e.g.[32–36]). In this paper, we have used Caputo fractional operator which is the most common one within physicists and scientists, it has a key advantage that the fractional derivative of constants are equal to zero. The significance of using the FDOs due to is eligible for capturing memory effects because of their non local nature. Therefore, FDOs are an appropriate tool to describe biological and epidemic models to predict the spread of diseases, controlling of the transmission of these diseases and so much more [37–42]. Since the emergence of COVID-19, many researchers have been dedicated to their efforts to forecasting the inflection point and terminating this disease in order to assist policymakers concerning the different actions that have been taken by different governments, and among these efforts is to provide mathematical models in order to understand the nature and transmission of this epidemic and design effective strategies to control it. A numerous of fractional-order mathematical models have developed and studied by many researchers to analyse the spreading outbreak of COVID-19 such as, in [43], proposed a fractional dynamic system for the COVID-19 epidemic contain eight population classes, five of them describe the infected cases depending on the detection and appearance of symptoms. The transmission of COVID-19 in Wuhan China modeled by a fractional mathematical model depended on Caputo-Fabrizio fractional derivative has been investigated [44], which split the population to five classes, susceptible, exposed, infected, recovered and concentration of COVID-19 in the surrounding environment. They used Adamas-Bashforth numerical scheme to solve this model and give their numerical simulations. The Caputo fractional-order derivative has used in a mathematical model to describe COVID-19 epidemic in [45], where the individuals are divided into five groups, susceptible, exposed, symptomatic infected, asymptomatic infected and removed (recovered and death) individuals. Also, they conducted a comparison between the results of the fractional-order model and the integer-order model with the real data which reported from around the world from January 22 to April 11 and from this comparison, they concluded that the values derived from the fractional derivative are closer to the real data, and have a less relative error. In [46], Sheikh et al. have investigated a Bats–Hosts–Reservoir–People transmission fractional-order COVID-19 model. The reported real data from India on 14 March 2000 to 26 March 2020 are presented, also various parameters estimated or fitted according to this real data. Other relevant studies for the modeling of COVID-19 can be seen in [47–57].

Motivated by the investigations mentioned above, specially the work of Zu et al. [15], and the current situation of COVID-19, the main contribution of the present work is to find a good strategy to trace the Pandemic trend and reduce the transmission risk based on the fractional mathematical model. First, we have simulated the proposed model with it's fractional order based on the reported parameters in [15], from which we conclude the need of using fractional order and re-estimate the parameters again. Then, Simulations of the proposed model in it's fractional order with the new estimated parameters are presented together with the real data. The organization of this paper as follows. In Section 2, we formulate the FOM for COVID-19. In Section 3, we discuss the equilibrium points (EPs) and analyzed their stability with the help of the effective reproduction number. Section 4 is devoted to give numerical simulations for the proposed model and an adequate explanation of our results with various values of the fractional order and comparing it with the real data. Summarizing the results of this paper will be provided in Section 5.

2. Mathematical formulation of the FOM

The mathematical model considered in [15] describes COVID-19 as a system of ODEs. Here, we introduced a more generalized model that is governed by a system of fractional differential equations (FDEs) with Caputo fractional derivative of order $0 < \alpha \leqslant 1$, which is defined as [29,34]

$$ {}_0{}^{C}\mathfrak{D}_{\xi}^{\alpha} f(\xi) = \frac{1}{\Gamma(1-\alpha)} \int {}_0{}^{\xi}(\xi - t)^{-\alpha} f'(t)dt, $$

where f is a given function and $\Gamma(.)$ denotes the gamma function. It is known that ${}_0{}^{C}\mathfrak{D}_{\xi}^{\alpha} f(\xi) \longrightarrow f'(t)$ as $\alpha \longrightarrow 1$. Then, the proposed FOM reads:

$$ \begin{aligned} {}_0{}^{C}\mathfrak{D}_{\xi}^{\alpha} S(\xi) = &- \frac{(1-\rho)\beta C_r S(\xi)}{N}(\beta_1 L(\xi) + I(\xi)) - \frac{(1-\beta)\rho C_r S(\xi)}{N}(\beta_1 L(\xi) + I(\xi)) \\ &- \frac{\rho\beta C_r S(\xi)}{N}(\beta_1 L(\xi) + I(\xi)) - kD(\xi) + k_1 P(\xi) + \lambda S_\rho(\xi), \end{aligned} \tag{1} $$

$$ {}_0{}^{C}\mathfrak{D}_{\xi}^{\alpha} S_\rho(\xi) = \frac{(1-\beta)\rho C_r S(\xi)}{N}(\beta_1 L(\xi) + I(\xi)) - \lambda S_\rho(\xi), \tag{2} $$

$$ {}_0{}^{C}\mathfrak{D}_{\xi}^{\alpha} L(\xi) = \frac{(1-\rho)\beta C_r S(\xi)}{N}(\beta_1 L(\xi) + I(\xi)) - (k_2 + \epsilon)L(\xi), \tag{3} $$

$$ {}_0{}^{C}\mathfrak{D}_{\xi}^{\alpha} L_\rho(\xi) = \frac{\rho\beta C_r S(\xi)}{N}(\beta_1 L(\xi) + I(\xi)) - k_2 L_\rho(\xi), \tag{4} $$

$$ {}_0{}^{C}\mathfrak{D}_{\xi}^{\alpha} I(\xi) = \epsilon L(\xi) - (k_3 + \delta)I(\xi), \tag{5} $$

$$ {}_0{}^{C}\mathfrak{D}_{\xi}^{\alpha} P(\xi) = kD(\xi) + k_2(L_\rho(\xi) + L(\xi)) - (k_1 + k_4)P(\xi), \tag{6} $$

$$ {}_0{}^{C}\mathfrak{D}_{\xi}^{\alpha} D(\xi) = k_4 P(\xi) - (\gamma + \delta)D(\xi) + k_3 I(\xi), \tag{7} $$

$$ {}_0{}^{C}\mathfrak{D}_{\xi}^{\alpha} R(\xi) = \gamma D(\xi), \tag{8} $$

$$ {}_0{}^{C}\mathfrak{D}_{\xi}^{\alpha} X(\xi) = k_3 I(\xi) + k_4 P(\xi), \tag{9} $$

Table 1
Meaning and values of the parameters in the FOM (1)-(11) as well as the ICs.

Parameter	Description	Value	Ref.
ρ	The quarantined rate of close contacts	0.2432	Fitted
β	The transmission rate	0.0977	Fitted
β_1	The relative transmission strength of $L(\xi)$ to $I(\xi)$	0.1914	Fitted
C_r	The Contact rate	$C_r = c_1 + c_2 e^{-c_3\xi}$	[15]
$c_i, i = 1,2,3$	Positive real constants to compute C_r	0.0393, 17.263, 0.118	Fitted
k	The transfer rate from $S(\xi)$ to $P(\xi)$	1.7718e-04	Fitted
k_1	The transfer rate from $P(\xi)$ to $S(\xi)$	0.1286	Fitted
k_2	The transfer rate from $L(\xi)$ to $P(\xi)$	0.1743	Fitted
k_3	The transfer rate from $I(\xi)$ to $D(\xi)$	0.1762	Fitted
k_4	The transfer rate from $P(\xi)$ to $D(\xi)$	0.0560	Fitted
λ	The release rate from $S_\rho(\xi)$ to $S(\xi)$	1/14	[15,58]
ϵ	The transfer rate from $L(\xi)$ to $I(\xi)$	1/5.2	[15,59]
δ	The death rate due to infection	0.0021	Fitted
γ	The recovery rate from $D(\xi)$ to $R(\xi)$	0.0425	Fitted
$L(0)$	The initial value of $L(\xi)$	7.6322e + 03	Fitted
$I(0)$	The initial value of $I(\xi)$	1.1143e + 03	Fitted
$L_\rho(0)$	The initial value of $L_\rho(\xi)$	69.3904	Fitted
$S(0)$	The initial value of $S(\xi)$	1.3371e + 09	Fitted
$S_\rho(0)$	The initial value of $S_\rho(\xi)$	591.8880	Fitted
$P(0)$	The initial value of $P(\xi)$	2.7832e + 03	Fitted

$$ {}_0{}^C\mathfrak{D}_\xi^\alpha Y(\xi) = k_2(L(\xi) + L_\rho(\xi)) + kD(\xi), \tag{10} $$

$$ {}_0{}^C\mathfrak{D}_\xi^\alpha Z(\xi) = \delta(I(\xi) + D(\xi)), \tag{11} $$

where the total population N is divided into eight components, namely; S describes the susceptible individuals in the free environment, L be the latent individuals, L_ρ be the traced latent individuals, P be the suspected individuals, D be the diagnosed individuals, S_ρ characterizes the traced susceptible individuals who had direct contact with diagnosed or suspected individuals, I be the infectious individuals in the free environment and R be the recovered individuals. In addition, we took into consideration the cumulative number of confirmed cases X, the cumulative number of suspected cases Y and the cumulative number of deaths Z. The meaning of the parameters and the ICs for the FOM are given in Table 1.

3. Stability of the EPs

In this section, we explore the stability for the FOM by considering the disease free equilibrium, the effective reproduction number $\mathscr{R}_0$ and the endemic equilibrium.

(i) A disease-free equilibrium (DFE) point:

We shall use only the Eqs. (1)–(7) of the FOM to find the EPs. The model equilibria is obtained here by assuming

$$ \begin{cases} {}_0{}^C\mathfrak{D}_\xi^\alpha S(\xi) = 0, \ {}_0{}^C\mathfrak{D}_\xi^\alpha S_\rho(\xi) = 0, \ {}_0{}^C\mathfrak{D}_\xi^\alpha L(\xi) = 0, \ {}_0{}^C\mathfrak{D}_\xi^\alpha L_\rho(\xi) = 0, \\ {}_0{}^C\mathfrak{D}_\xi^\alpha I(\xi) = 0, \ {}_0{}^C\mathfrak{D}_\xi^\alpha P(\xi) = 0, \ {}_0{}^C\mathfrak{D}_\xi^\alpha D(\xi) = 0, \end{cases} \tag{12} $$

by solving Eqs. (12), then the DFE for the FOM is

$\Xi_0 = (S^{eq}, 0, 0, 0, 0, 0, 0)$.

Following [60], in order to derive the expression of $\mathscr{R}_0$, the choice of the necessary computations of the matrices F and V, which is epidemiologically correct, are given as

$$ F = \begin{bmatrix} 0 & \beta_1 F_1 S^{eq} & 0 & F_1 S^{eq} & 0 & 0 \\ 0 & \beta_1 F_2 S^{eq} & 0 & F_2 S^{eq} & 0 & 0 \\ 0 & \beta_1 F_3 S^{eq} & 0 & F_3 S^{eq} & 0 & 0 \\ 0 & \epsilon & 0 & 0 & 0 & 0 \\ 0 & k_2 & k_2 & 0 & 0 & k_1 \\ 0 & 0 & 0 & k_3 & k_4 & 0 \end{bmatrix}, $$

and

$$ V = \begin{bmatrix} \lambda & 0 & 0 & 0 & 0 & 0 \\ 0 & k_2 + \epsilon & 0 & 0 & 0 & 0 \\ 0 & 0 & k_2 & 0 & 0 & 0 \\ 0 & 0 & 0 & k_3 + \delta & 0 & 0 \\ 0 & 0 & 0 & 0 & k_1 + k_4 & 0 \\ 0 & 0 & 0 & 0 & 0 & \gamma + \delta \end{bmatrix}, $$

where

$$ \begin{aligned} F_1 &= \frac{(1-\beta)\rho C_r}{N}, \\ F_2 &= \frac{(1-\rho)\beta C_r}{N}, \\ F_3 &= \frac{\rho\beta C_r}{N}. \end{aligned} \tag{13} $$

Then, the spectral radius of FV^{-1} is the required effective reproduction number of the FOM which is given by

$$ \mathscr{R}_0 = \frac{\beta_1 F_2 S^{eq}}{2(k_2+\epsilon)} + \frac{1}{2}\sqrt{\left(\frac{\beta_1 F_2 S^{eq}}{k_2+\epsilon}\right)^2 + 4\frac{F_2 \epsilon S^{eq}}{(k_2+\epsilon)(k_3+\delta)}}. \tag{14} $$

Theorem 3.1. The equilibrium Ξ_0 of the system (1)-(7) is asymptotically stable if $\mathscr{R}_0 < 1$. **Proof.** We compute the Jacobian matrix at DFE Ξ_0 as follow:

$$ J_{\Xi_0} = \begin{bmatrix} -\lambda & \beta_1 F_1 S^{eq} & 0 & F_1 S^{eq} & 0 & 0 \\ 0 & \beta_1 F_2 S^{eq} - (k_2+\epsilon) & 0 & F_2 S^{eq} & 0 & 0 \\ 0 & \beta_1 F_3 S^{eq} & -k_2 & F_3 S^{eq} & 0 & 0 \\ 0 & \epsilon & 0 & -(k_3+\delta) & 0 & 0 \\ 0 & k_2 & k_2 & 0 & -(k_1+k_4) & k \\ 0 & 0 & 0 & k_3 & k_4 & -(\gamma+\delta) \end{bmatrix}. $$

By calculating the eigenvalues of J_{Ξ_0}, we have $\chi_1 = -\lambda < 0, \chi_2 = -k_2 < 0$ and the rest eigenvalues are given as follows:

$$ \chi^2 + A_1\chi + B_1 = 0, \tag{15} $$

where

$$ \begin{aligned} &A_1 = k_1 + k_4 + \gamma + \delta; A_1 \text{isalwayspositive}, \\ &B_1 = (k_1 + k_4)(\gamma + \delta) - kk_4. \end{aligned} \tag{16} $$

The last two eigenvalues are obtained through the following quadratic equation:

$$ \chi^2 + A_2\chi + B_2 = 0, \tag{17} $$

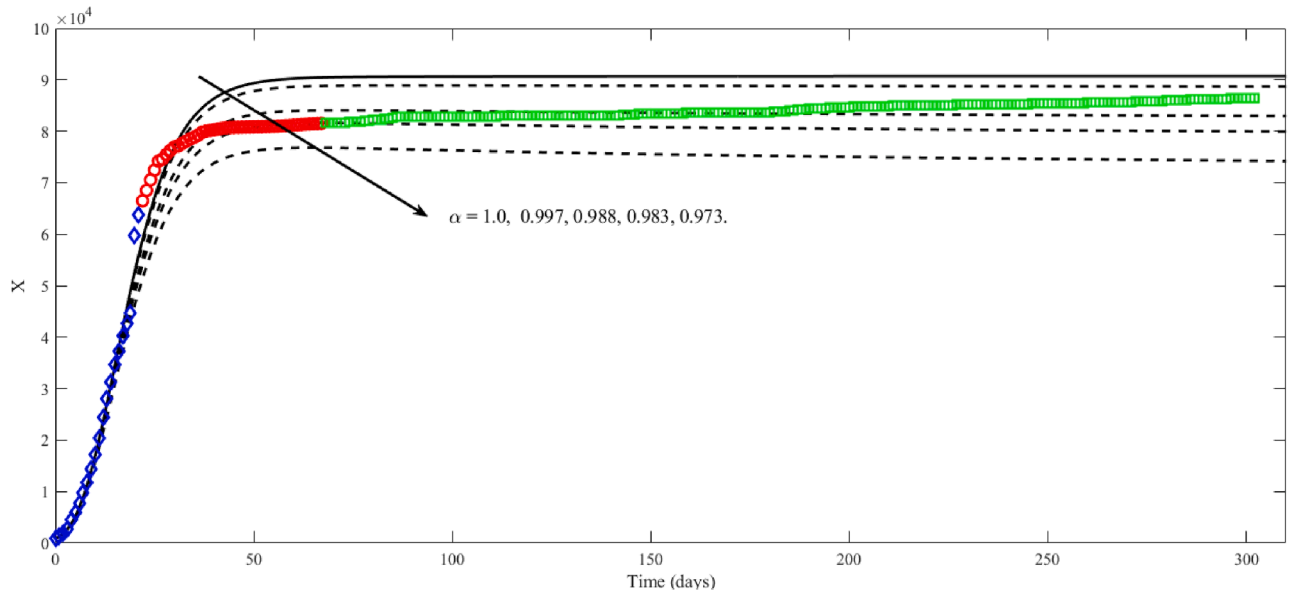

(a)

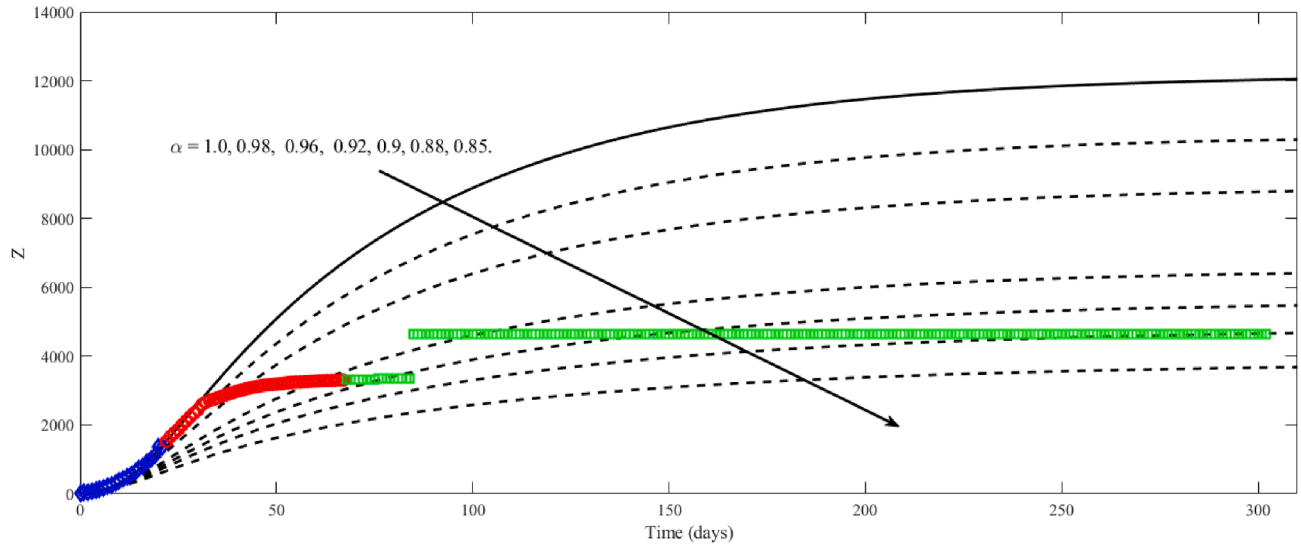

(b)

Fig. 1. Influence of the cumulative number of (a) confirmed cases and (b) deaths via time obtained using the parameters tabulated in [15] and estimated base on the actual values of blue diamond-shaped while red circle-shaped and green square-shaped are the actual values presented for the sake of checked the simulation of that case (motivation of the fractional model).

where

$$A_2 = k_2 + \epsilon - \beta_1 F_2 S^{eq} + k_3 + \delta,$$
$$B_2 = (k_2\epsilon - \beta_1 F_2 S^{eq})(k_3 + \delta) - \epsilon F_2 S^{eq}. \tag{18}$$

From Eq. (16) and Eq. (18), we can observe that.

- For asymptotically stable, it must be $B_1 > 0$ in Eq. (15), which means that $(k_1 + k_4)(\gamma + \delta) > kk_4$.
- The coefficients A_2, B_2 of Eq. (17) have positive signal whenever $\mathscr{R}_0 < 1$.
- The stability of the DFE depends on the signal of B_1.

Remark 3.1. If all coefficients of polynomials (15) and (17) have the same signal (positive), then the eigenvalues have negative real part (see, e.g. [61]). Consequently, the DFE is asymptotically stable, if $B_1 > 0$ and $\mathscr{R}_0 < 1$. □

(ii) An endemic equilibrium point:

We denote the endemic equilibrium point by Ξ^*, which is given when there is an infection I^*.

$$\Xi^* = (S^*, S^*_\rho, L^*, L^*_\rho, I^*, P^*, D^*),$$

where the values of $S^*, S^*_\rho, L^*, L^*_\rho, P^*, D^*$ are obtained as follows:

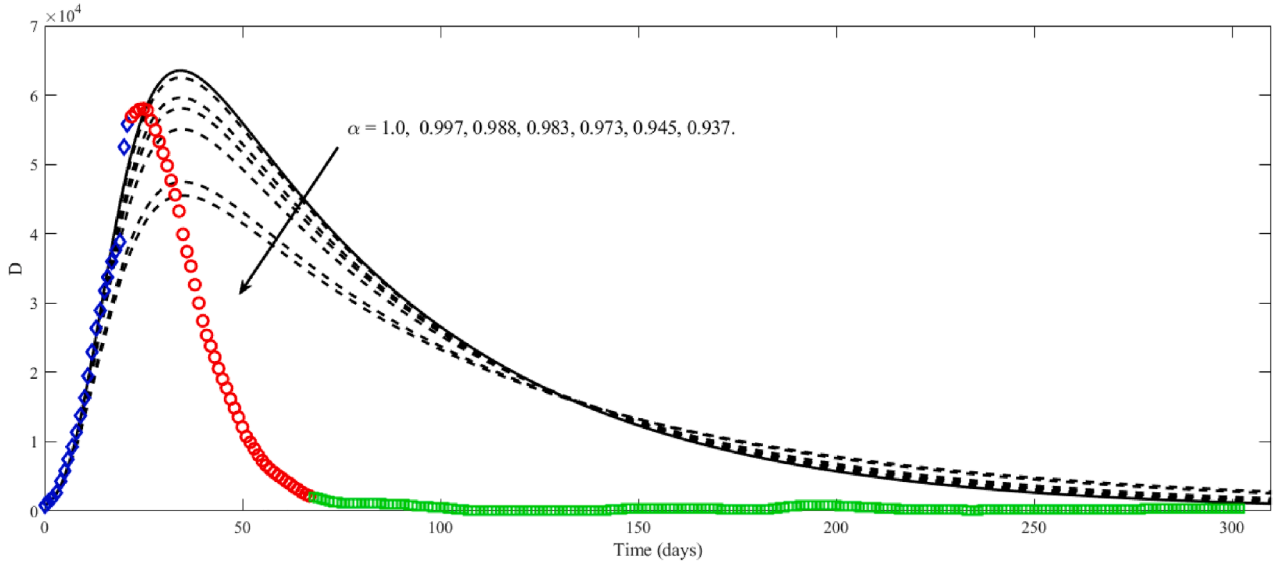

(a)

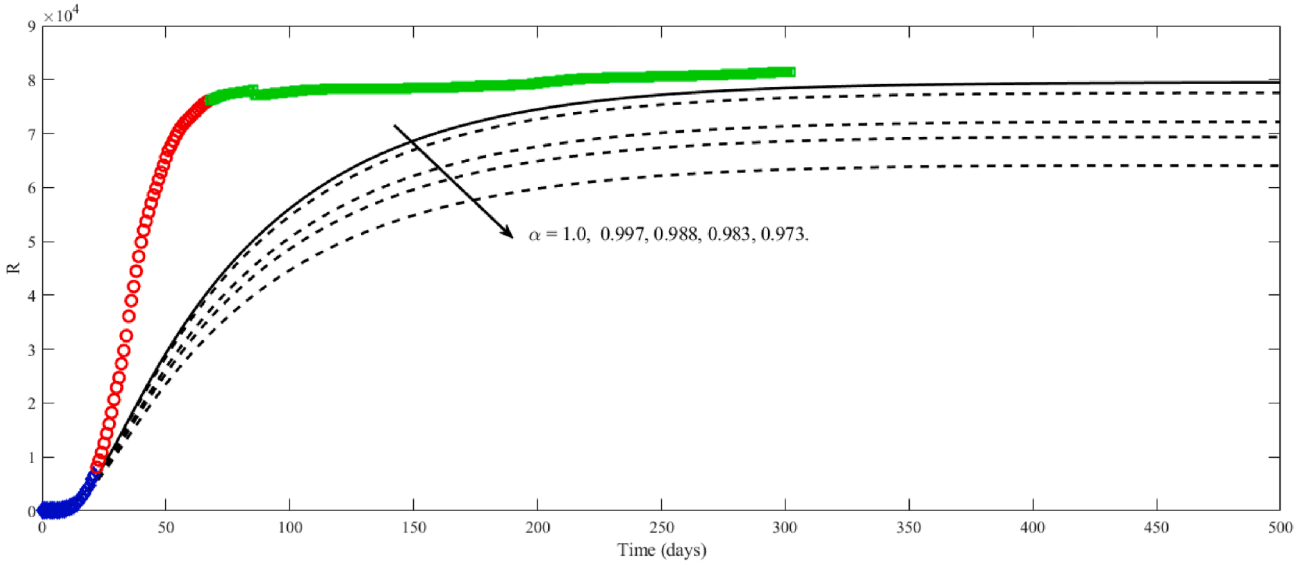

(b)

Fig. 2. Influence of number of the (a) existing confirmed cases and (b) cumulative recovered cases along time obtained using the parameters tabulated in [15] and estimated base on the actual values of blue diamond-shaped while red circle-shaped and green square-shaped are the actual values presented for the sake of checked the simulation of that case (drawback of the old estimated parameters).

$$\begin{cases} S^* = \dfrac{(k_3+\delta)(k_2+\epsilon)}{F_2(\beta_1(k_3+\delta)+\epsilon)}, \\ S_\rho^* = \dfrac{\rho(1-\beta)(k_3+\delta)(k_2+\epsilon)}{\epsilon\beta\lambda(1-\rho)} I^*, \\ L^* = \dfrac{(k_3+\delta)}{\epsilon} I^*, \\ L_\rho^* = \dfrac{\rho(k_3+\delta)(k_2+\epsilon)}{\epsilon k_2(1-\rho)} I^*, \\ P^* = \dfrac{\epsilon k k_3(1-\rho)+(k_3+\delta)(\gamma+\delta)(\epsilon\rho+k_2)}{\epsilon(1-\rho)[(k_1+k_4)(\gamma+\delta)-kk_4]} I^*, \\ D^* = \dfrac{1}{\gamma+\delta}\left[k_3 + k_4 \dfrac{\epsilon k k_3(1-\rho)+(k_3+\delta)(\gamma+\delta)(\epsilon\rho+k_2)}{\epsilon(1-\rho)[(k_1+k_4)(\gamma+\delta)-kk_4}\right] I^*. \end{cases} \tag{19}$$

Now, we end this section by proving the following theorem of the stability of Ξ^* when the basic reproduction number Eq. (14) is greater than one.

Theorem 3.2. If $\mathscr{R}_0 > 1$, then the unique positive endemic equilibrium Ξ^* of the system (1)-(7) is marginally stable. **Proof.** The Jacobian matrix at Ξ^* is given by

$$J_{\Xi^*} = \begin{bmatrix} -\lambda & \dfrac{\beta_1 F_1(k_3+\delta)(k_2+\epsilon)}{F_2(\beta_1(k_3+\delta)+\epsilon)} & 0 & \dfrac{F_1(k_3+\delta)(k_2+\epsilon)}{F_2(\beta_1(k_3+\delta)+\epsilon)} & 0 & 0 \\ 0 & \dfrac{\beta_1(k_3+\delta)(k_2+\epsilon)}{(\beta_1(k_3+\delta)+\epsilon)} - (k_2+\epsilon) & 0 & \dfrac{(k_3+\delta)(k_2+\epsilon)}{(\beta_1(k_3+\delta)+\epsilon)} & 0 & 0 \\ 0 & \dfrac{\beta_1 F_3(k_3+\delta)(k_2+\epsilon)}{F_2(\beta_1(k_3+\delta)+\epsilon)} & -k_2 & \dfrac{F_3(k_3+\delta)(k_2+\epsilon)}{F_2(\beta_1(k_3+\delta)+\epsilon)} & 0 & 0 \\ 0 & \epsilon & 0 & -(k_3+\delta) & 0 & 0 \\ 0 & k_2 & k_2 & 0 & -(k_1+k_4) & k \\ 0 & 0 & 0 & k_3 & k_4 & -(\gamma+\delta) \end{bmatrix},$$

where F_1, F_2, F_3 are given by Eqs. (13). Then the eigenvalues of J_{Ξ^*} are $\varkappa_1 = 0, \varkappa_2 = -\lambda < 0, \varkappa_3 = -k_2 < 0, \varkappa_4 = -\left(\frac{\epsilon(k_2+\epsilon)}{\beta_1(k_3+\delta)+\epsilon} + k_3 + \delta\right) < 0$ and the eigenvalues $\varkappa_5, \varkappa_6$ are also negative, where these eigenvalues can be obtained by solving a quadratic equation w.r.t $\varkappa$, which has the same coefficients of Eq. (15). Briefly, we have one of the eigenvalues is zero and the others are negative, whenever $\mathscr{R}_0 > 1$, thus the FOM will be marginally stable.□

4. Simulation of the FOM

This section is devoted to give a deep understanding of the numerical simulations of the considered model together with some interpretation of the obtained results. By the end of this section, we have a clear answer to the motivation of the use of the fractional model. The FOM (1)-(11) is solved numerically together with a set of the ICs and parameters in Table 1. Multi step Adams–Bashforth-Moulton is adapted for this purpose. Indeed, this method has been widely used and its accuracy and convergence have been studied well in [62–64].

In Figs. 1 and 2, we simulate the FOM (1)-(11) using the same estimated ICs and parameters reported in [15]. The values of the reported data of group I are shown in blue diamond-shaped and those of group II are in red circle-shaped, whereas the green square-shaped represents those in group III. The estimated parameters in [15] were obtained based on the reported data from the NHC of China for the period from 23 rdof January to 13rdof February 2020 (Group I in Table 2, Appendix A). In those figures, the new reported data from 14thof February to 30thof March 2020 (red circle) as well as those from 31 st of March till 21st of November 2020 (green square-shaped) are added for the sake of comparison. Moreover, for the convenient of the reader, those data (from the NHC of China) are listed in Table 2, in group II and group II, respectively. Different values for the fractional derivatives are simulated in Figs. 1 and 2, from which one could find that as the time increases the model should be considered in its fractional form. This result make the benefits of considering our proposed model as in (1)-(11). Moreover, by examine Fig. 2, we concluded that the reported parameters in [15], for the days from 23 rdof January to 13rdof February 2020 (Group I in Table 2), have to be re-estimated using more real data. Then, data of group I together with those of group II have been used in order to re-estimate the new parameters based on the same method as in [15]. These new parameters and ICs are reported in Table 1, and they are used for the remaining simulations.

As in Section 3, the R_0 of COVID-19 is given by Eq.(14), which is approximated to equal 2.252 on January 23, 2020 ($t = 0$) in case of using the new re-estimated parameters from Table 2. The influence of this number along time is illustrated in Fig. 3 for both the current results and those reported in [15]. From Fig. 3, there is a bit quantitative difference in the values of the reproduction number obtained from the current study and that of [15]. Both of them have the same behavior and the main point here is that none of them increases again after dropped below 1.0. These results have a direct connection to the stability of the model as shown in Section 3. Moreover, after February 6, 2020, the reproduction number had dropped below 1.0, which proposed that the number of the new infections would gradually decreases from that date. The verification of this behavior could be seen also from Fig. 4, where the number of infections in the free environment decreases after reaching to its high peak for all the chosen values of α.

Fig. 5 presents the influence of the cumulative number of the confirmed cases with various values of α. As mentioned above, the last group was used for the purpose of checking the behavior of the proposed model with the fitted valued obtained using group I and II. Thus, group III was not counted to the estimation process. As seen from Fig. 5, the green square-shaped valued are shown in the curve for $\alpha \in [0.973, 0.983]$. Within this interval, we have the best values of α for the

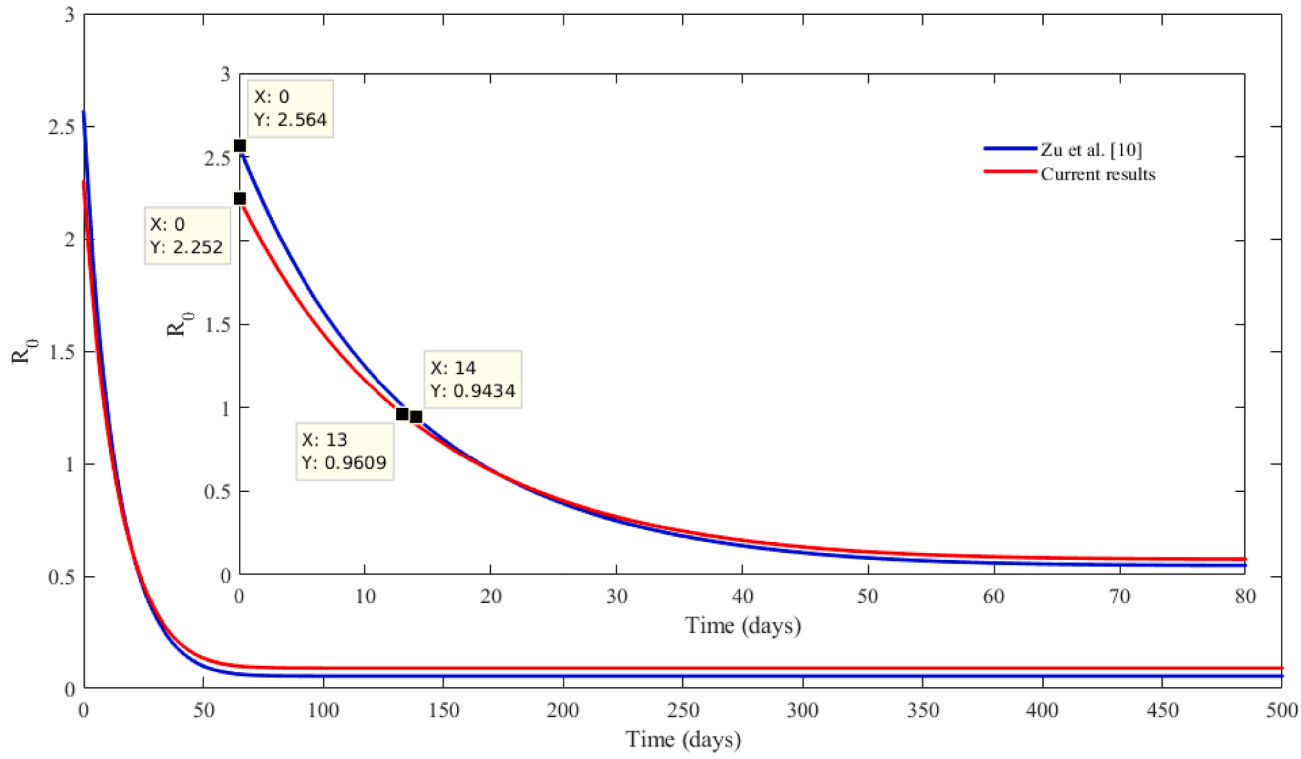

Fig. 3. Influence of the reproduction number R_0 along time for the current result and that obtained by Zu et al. [15].

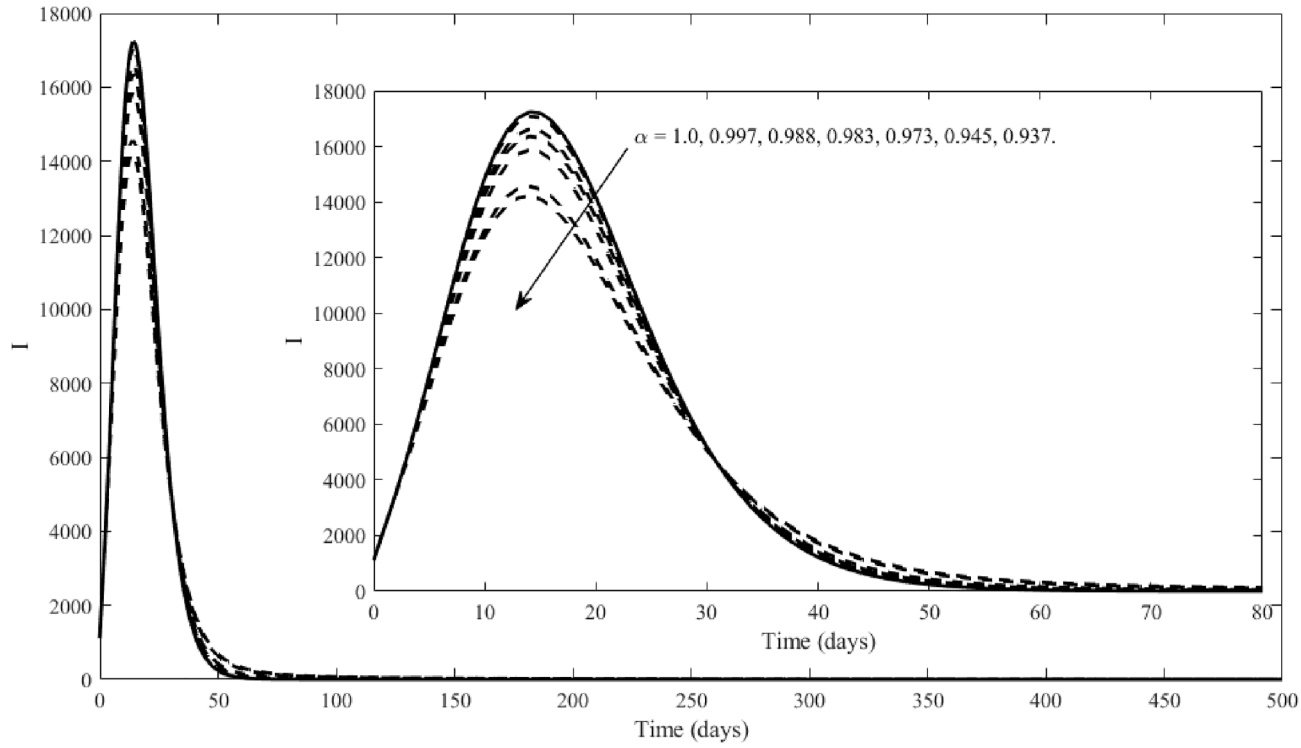

Fig. 4. Influence of the infectious individuals in the free environment I along time.

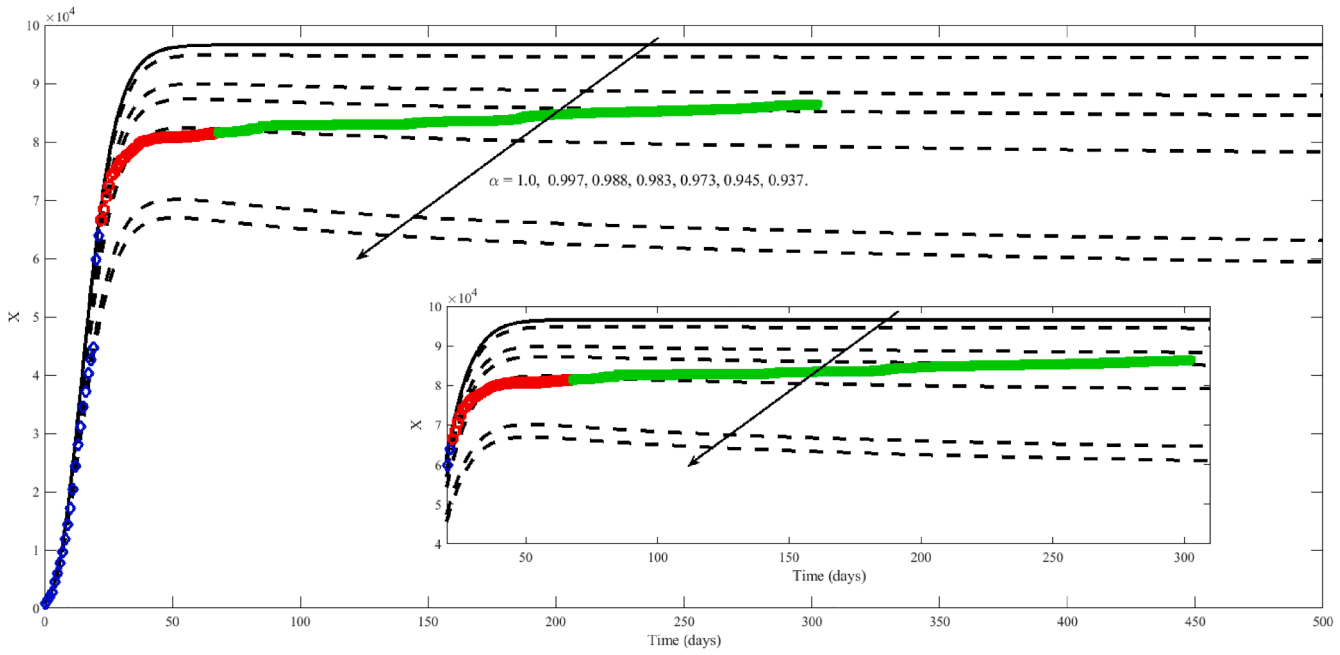

Fig. 5. Influence of the cumulative number of confirmed cases along time with various values of α. Blue diamond-shaped and red circle-shaped are the actual values used for fitting the parameters while the green square-shaped are actual data to examine the numerical simulations of the model.

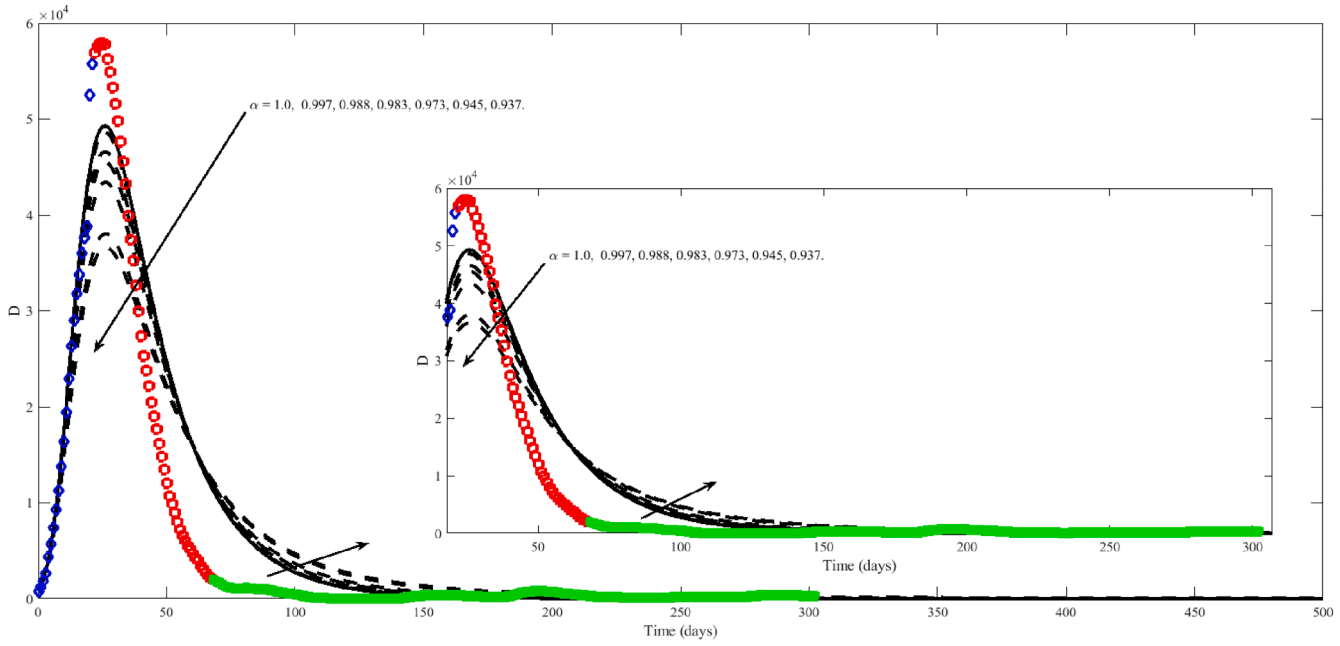

Fig. 6. Influence of the existing confirmed cases along time with various values of α. Blue diamond-shaped and red circle-shaped are the actual values used for fitting the parameters while the green square-shaped are actual data to examine the numerical simulations of the model.

proposed model in order to accurately predict the quantitative behavior of the cumulative number of the confirmed cases with time. Moreover, simulation for the flow of the existing confirmed cases along time is presented in Fig. 6 with various values of α. The number of the existing confirmed cases increases till it reaches to the peak after 29 days from the starting point in 23 of January, 2020. Then those numbers decrease for all the values of αas well as those reported data. The reported data are a bit less than those obtained from the simulation of the model. This slight difference could be interpreted due to the human effects that are not incorporated to our model. After a certain time, people become more sensitive to the epidemic of COVID-19 as it becomes a global pandemic and therefore they become very keen about the necessary safety precautions. Also, it should be noted the difference comparing this plot with that of Fig. 2(a).

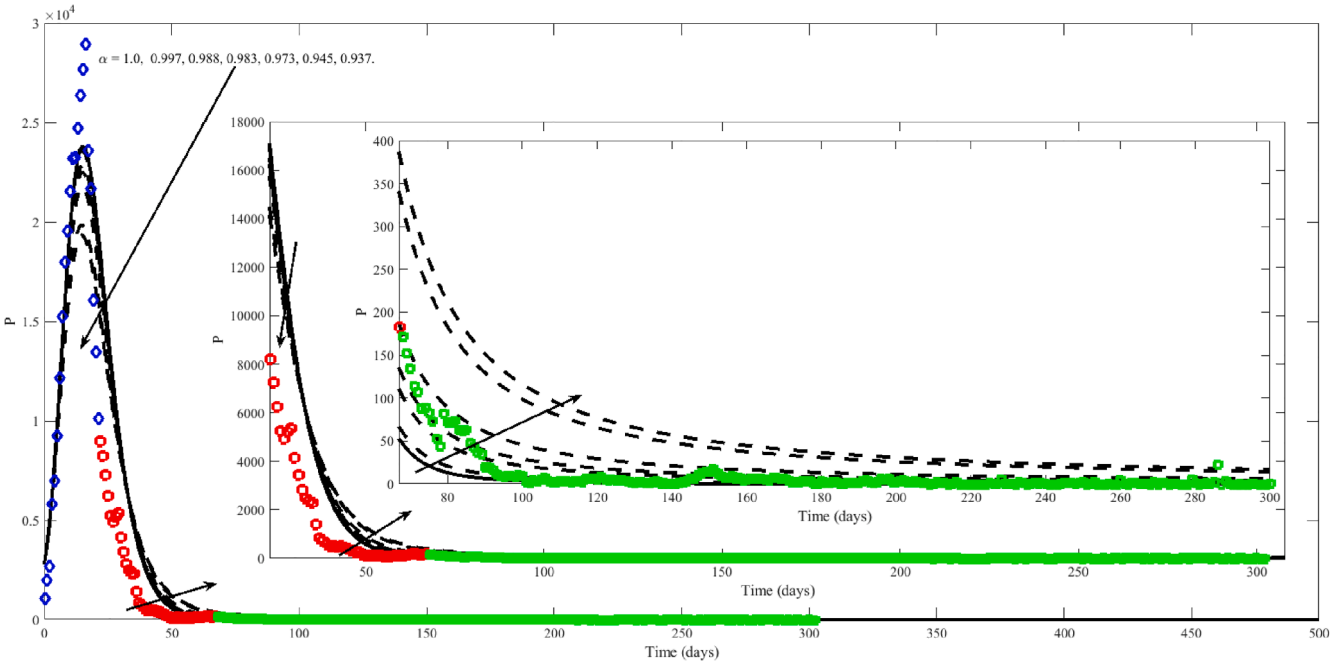

Fig. 7. Influence of the existing suspected cases along time with various values of α. Blue diamond-shaped and red circle-shaped are the actual values used for fitting the parameters while the green square-shaped are actual data to examine the numerical simulations of the model.

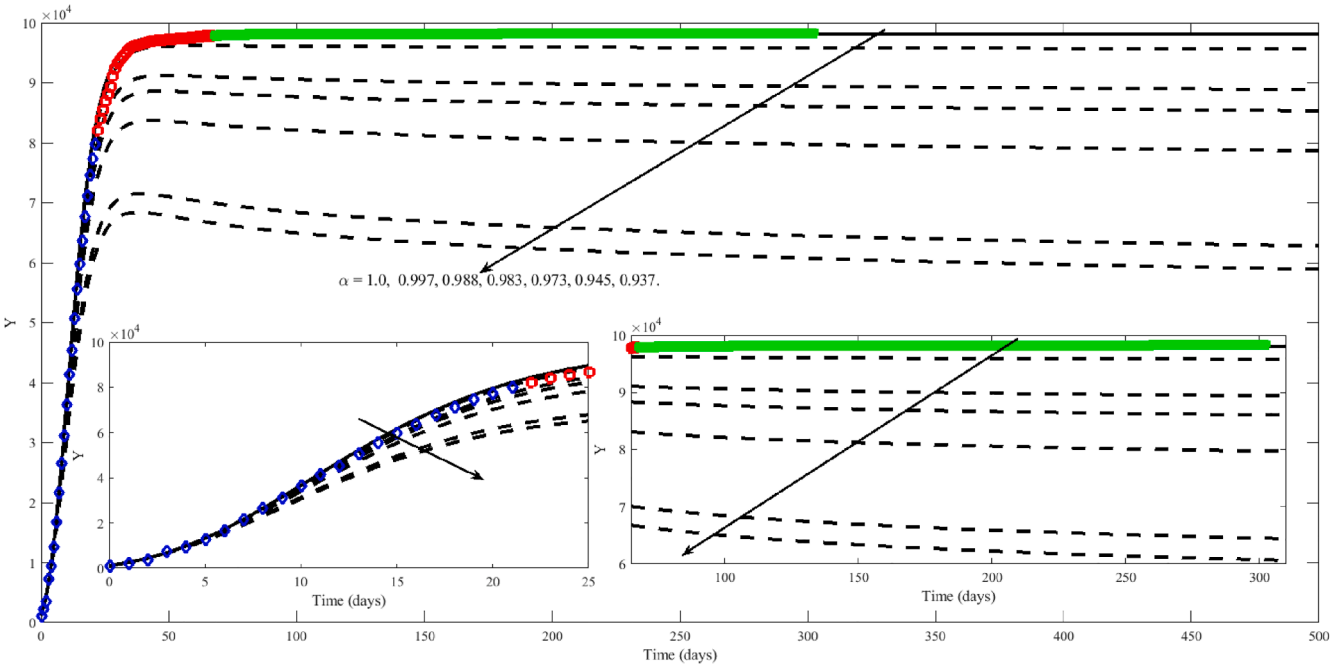

Fig. 8. Influence of the cumulative suspected cases along time with various values of α. Blue diamond-shaped and red circle-shaped are the actual values used for fitting the parameters while the green square-shaped are actual data to examine the numerical simulations of the model.

The influence of the existing suspected cases along time for various values of α is illustrated in Fig. 7. As time involves, the number of the existing suspected cases decreases for all the values of α. It is found that when $\alpha \geqslant 0.973$ (as seen in the second zoom in of the plot), one could gain a better prediction of the number of the existing suspected cases along time. In addition, simulation of the cumulative suspected cases along time is plotted in Fig. 8 for various values of α. From those green values, it seems that when time evolves the best value of α, for this case, converges to 1.0. Fig. 9 indicates the influence of the number of the existing medical observations; $S_\rho + L_\rho$ along time. As it can be seen from this plot

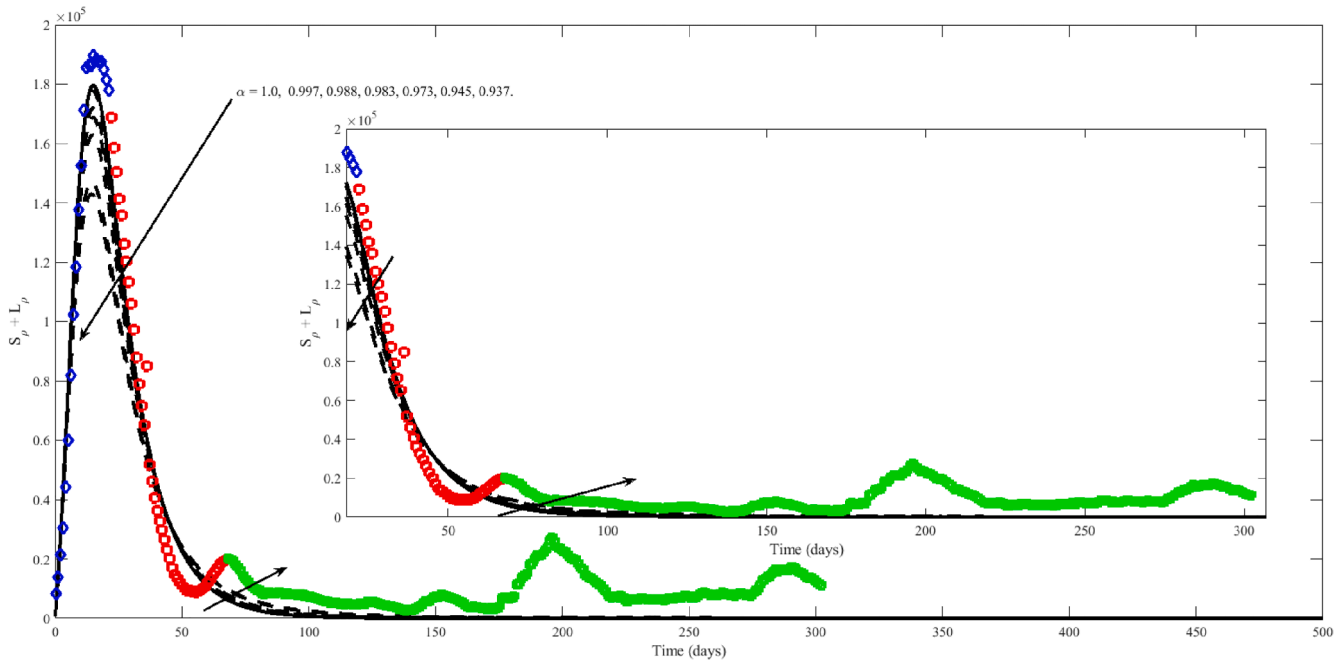

Fig. 9. Influence of the existing medical observations along time with various values of α. Blue diamond-shaped and red circle-shaped are the actual values used for fitting the parameters while the green square-shaped are actual data to examine the numerical simulations of the model.

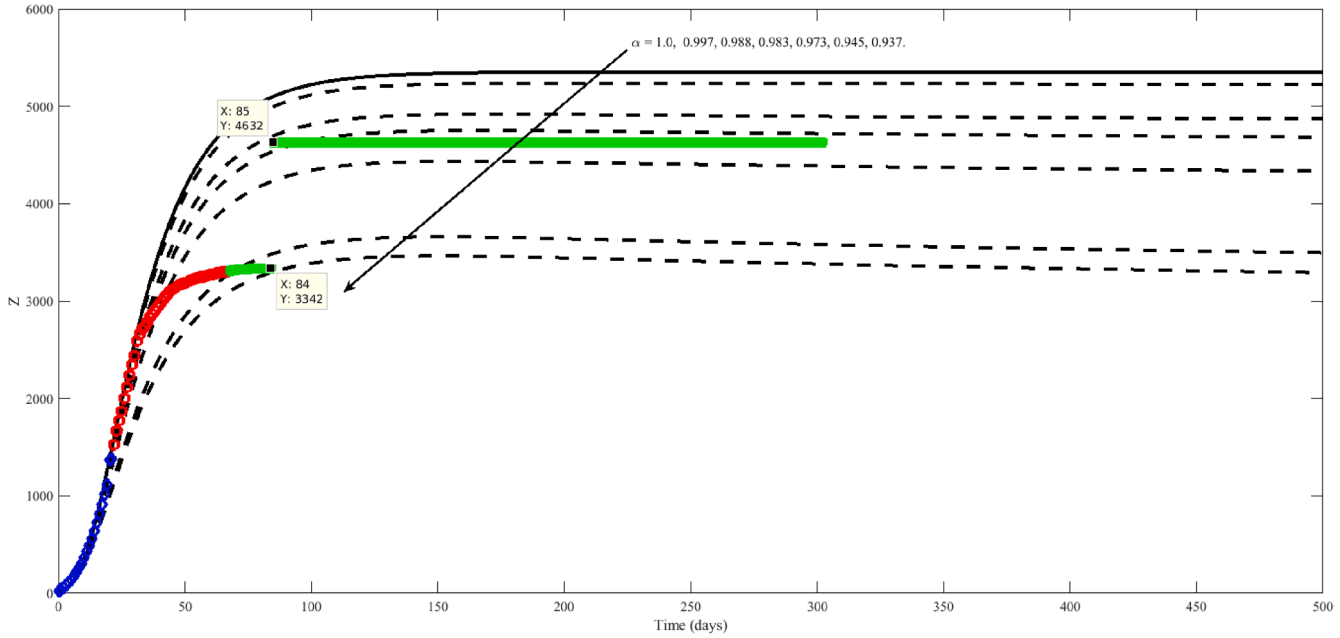

Fig. 10. Influence of the cumulative deaths along time with various values of α. Blue diamond-shaped and red circle-shaped are the actual values used for fitting the parameters while the green square-shaped are actual data to examine the numerical simulations of the model.

the recorded data start increasing till a certain peak then decreases again. Later with evolving time it gains a wavy diffusion effect with a small amplitude. The obtained results from the model are similar except for the last diffusion effect, i.e. it has a damped wave effect. Influence of the cumulative number of deaths along time with various values of α is given in Fig. 10. The actual data are close to the simulated curve corresponding to law values of α, till day 16 April 2020. In the next day, 17 April 2020, there is a big jump on the actual data corresponding to the death of 1290 person, which, from that day and on, coincide with the simulation of the model for $\alpha = 0.983$. This behaviour in the actual data

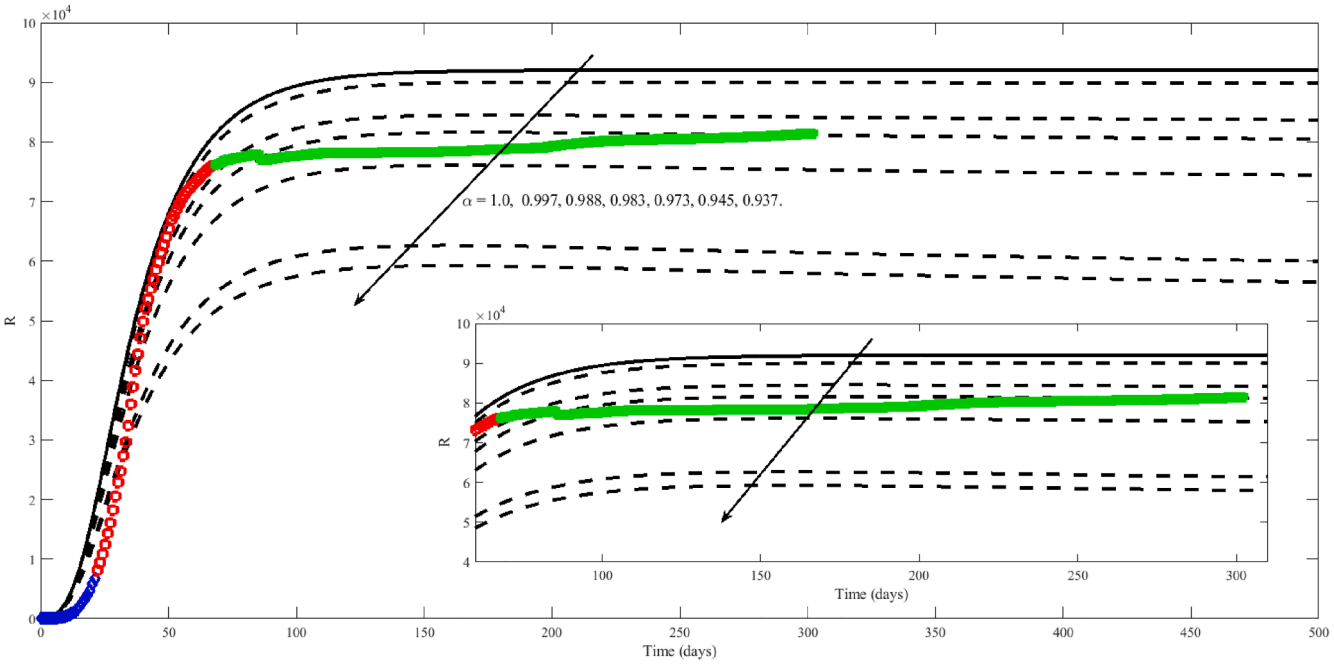

Fig. 11. Influence of the cumulative recovered cases along time with various values of α. Blue diamond-shaped and red circle-shaped are the actual values used for fitting the parameters while the green square-shaped are actual data to examine the numerical simulations of the model.

is going to affect the behaviour of the commutative number of the recovered cases shown in Fig. 11. As it can be seen from that figure, there is a decay in the commutative actual data corresponding to death numbers. Comparing the resulting simulations of Fig. 11 with those of Fig. 2(b), the improvement in the results of the current study would be very clear. It is found that, if $\alpha \in [0.973, 0.988]$, a better prediction for R could be concluded. Overall, an alternative method based on the fractional order of the model is presented here for a better prediction of the behavior of COVID-19, which do affect the propagation of the COVID-19.

5. Conclusion

In the present work, we managed to propose a COVID-19 model of fractional order α (where $0 < \alpha \leqslant 1$) in which a possessed memory is gained. Within the realistic data, reported in the NHC of China from January 23 till March 30, 2020, the estimated parameters of the model were introduced. The actual data from 31 of March till 21 November were used to check the resulting simulation of the FOM. The effective reproduction number R_0 has been computed and we showed the stability analysis of the disease free equilibria Ξ_0 and the endemic equilibrium Ξ^* of the proposed FOM on the basis of R_0. Numerical simulations for the components of the proposed model are displayed with various values of α and these solutions demonstrated our theoretical analysis for the FOM. From the simulations, the main finding is more arising where the FOM coincides with the real data that means it more accurate for the prediction of COVID-19 which leads to reduce the transmission risk of infection.

Authors contribution

Conceptualization: I. Ameen, H.M. Ali, M.R. Alharthi, A.H. Abdel-Aty, H.M. Elshehabey; Formal analysis: I. Ameen, H.M. Ali, H.M. Elshehabey; Investigation: I. Ameen, H.M. Ali, M.R. Alharthi, A.H. Abdel-Aty, H.M. Elshehabey; Methodology: I. Ameen, H.M. Ali, H.M. Elshehabey; Resources: H.M. Elshehabey, M.R. Alharthi, A.H. Abdel-Aty, I. Ameen, H.M. Ali; Software: I. Ameen, H.M. Ali, M.R. Alharthi, A.H. Abdel-Aty, H.M. Elshehabey; Supervision: I. Ameen, H.M. Ali, H.M. Elshehabey; Validation: I. Ameen, H.M. Ali, M.R. Alharthi, A.H. Abdel-Aty, H.M. Elshehabey; Writing - original draft: I. Ameen, H.M. Ali, M. R. Alharthi, A.H. Abdel-Aty, H.M. Elshehabey; Writing - review editing: all authors.

Declaration of Competing Interest

The authors declare that they have no known competing financial interests or personal relationships that could have appeared to influence the work reported in this paper.

Acknowledgments

Taif University Researchers Supporting Project number (TURSP-2020/275), Taif University, Taif, Saudi Arabia.

Appendix A. Appendix A

Table 2.

Table 2
Recorded data for COVID-19 in the mainland of China.

Groups	Date	X	P	Z	R	$S_\rho + L\rho$	Y	D
I	2020/1/23	830	–	25	34	8420	1072	771
	2020/1/24	1287	1965	41	38	13967	2190	1208
	2020/1/25	1975	2684	56	49	21556	3499	1870
	2020/1/26	2744	5794	80	51	30453	7305	2613
	2020/1/27	4515	6973	106	60	44132	9382	4349
	2020/1/28	5974	9239	132	103	59990	12630	5739
	2020/1/29	7711	12167	170	124	81947	16778	7417
	2020/1/30	9692	15238	213	171	102427	21590	9308
	2020/1/31	11791	17988	259	243	118478	26609	11289
	2020/2/1	14380	19544	304	328	137594	31171	13748
	2020/2/2	17205	21558	361	475	152700	36344	16369
	2020/2/3	20438	23214	425	632	171329	41416	1938
	2020/2/4	24324	23260	490	892	185555	45387	22942
	2020/2/5	28018	24702	563	1153	186354	50715	26302
	2020/2/6	31161	26359	636	1540	186045	55548	28985
	2020/2/7	34546	27657	722	2050	189660	59762	31774
	2020/2/8	37198	28942	811	2649	188183	63678	33738
	2020/2/9	40171	23589	908	3281	187518	67686	35982
	2020/2/10	42638	21675	1016	3996	187728	71222	37626
	2020/2/11	44653	16067	1113	4740	185037	74564	38800
	2020/2/12	59804	13435	1367	5911	181386	77371	52526
	2020/2/13	63851	10109	1380	6723	177984	79821	55748
II	2020/2/14	66492	8969	1523	8096	169039	82098	56873
	2020/2/15	68500	8228	1665	9419	158764	84016	57516
	2020/2/16	70548	7264	1770	10844	150539	85579	57934
	2020/2/17	72436	6242	1868	12552	141552	87011	58016
	2020/2/18	74185	5248	2004	14376	135881	88196	57805
	2020/2/19	74576	4922	2118	16155	126363	89473	56303
	2020/2/20	75465	5206	2236	18264	120302	91087	54965
	2020/2/21	76288	5365	2345	20659	113564	92448	53284
	2020/2/22	76936	4148	2442	22888	106089	93330	51606
	2020/2/23	77150	3434	2592	24734	97481	93950	49824
	2020/2/24	77658	2824	2663	27323	87902	94480	47672
	2020/2/25	78064	2491	2715	29745	79108	94919	45604
	2020/2/26	78497	2358	2744	32495	71572	95427	43258
	2020/2/27	78824	2308	2788	36117	65225	95879	39919
	2020/2/28	79251	1418	2835	39002	85233	96127	37414
	2020/2/29	79824	851	2870	41625	51856	96259	35329
	2020/3/1	80026	715	2912	44462	46219	96400	32652
	2020/3/2	80151	587	2943	47204	40651	96529	30004
	2020/3/3	80270	520	2981	49856	36432	96672	27433
	2020/3/4	80409	522	3012	52045	32870	96815	25352
	2020/3/5	80552	482	3042	53726	29869	96917	23784
	2020/3/6	80651	502	3070	55404	26730	97016	22177
	2020/3/7	80695	458	3097	57065	23074	97100	20533
	2020/3/8	80735	421	3119	58600	20146	97160	19016
	2020/3/9	80754	349	3136	59897	16982	97196	17721
	2020/3/10	80778	285	3158	61475	14607	97227	16145
	2020/3/11	80793	253	3169	62793	13701	97260	14831
	2020/3/12	80813	147	3176	64111	12161	97293	13526
	2020/3/13	80824	115	3189	65541	10879	97310	12094
	2020/3/14	80844	113	3199	66911	10189	97349	10734
	2020/3/15	80860	134	3213	67749	9582	97390	9898
	2020/3/16	80881	128	3226	68679	9351	97435	8976
	2020/3/17	80894	119	3237	69601	9222	97456	8056
	2020/3/18	80928	105	3245	70420	9144	97479	7263
	2020/3/19	80967	104	3248	71150	8989	97510	6569
	2020/3/20	81008	106	3255	71740	9371	97546	6013
	2020/3/21	81054	118	3261	72244	10071	97591	5549
	2020/3/22	81093	136	3270	72703	10701	97638	5120
	2020/3/23	81171	132	3277	73159	12077	97673	4735
	2020/3/24	81218	134	3281	73650	13356	97706	4287
	2020/3/25	81285	159	3287	74051	14714	97764	3947
	2020/3/26	81340	189	3292	74588	16005	97813	3460
	2020/3/27	81394	184	3295	74971	17198	97842	3128
	2020/3/28	81439	174	3300	75448	18581	97870	2691
	2020/3/29	81470	168	3304	75770	19235	97887	2396
	2020/3/30	81518	183	3305	76052	19853	97931	2161
III	2020/3/31	81554	172	3312	76238	20314	97957	2004
	2020/04/1	81589	153	3318	76408	20072	97977	1863
	2020/04/2	81620	135	3322	76571	19533	97989	1727
	2020/04/3	81639	114	3326	76755	18286	98000	1562
	2020/04/4	81669	107	3329	76964	17436	98011	1376

(*continued on next page*)

Table 2 (*continued*)

Groups	Date	X	P	Z	R	$S_\rho + L\rho$	Y	D
	2020/04/5	81708	88	3331	77078	16154	98021	1299
	2020/04/6	81740	89	3331	77167	14499	98033	1242
	2020/04/7	81802	83	3333	77279	13334	98045	1190
	2020/04/8	81865	73	3335	77370	12510	98062	1160
	2020/04/9	81907	53	3336	77455	11176	98065	1116
	2020/04/10	81953	44	3339	77525	10435	98073	1089
	2020/04/11	82052	82	3339	77575	9722	98122	1138
	2020/04/12	82160	72	3341	77663	9655	98128	1156
	2020/04/13	82249	72	3341	77738	8612	98131	1170
	2020/04/14	82295	73	3342	77816	8309	98142	1137
	2020/04/15	82341	63	3342	77892	8484	98146	1107
	2020/04/16	82367	62	3342	77944	8970	98149	1081
	2020/04/17	82719	63	4632	78029	8893	98154	1058
	2020/04/18	82735	48	4632	77062	8632	98156	1041
	2020/04/19	82747	43	4632	77084	8694	98158	1031
	2020/04/20	82758	37	4632	77123	8791	98161	1003
	2020/04/21	82788	35	4632	77151	8796	98164	1005
	2020/04/22	82798	20	4632	77207	8429	98164	959
	2020/04/23	82804	20	4632	77257	8362	98166	915
	2020/04/24	82816	17	4632	77346	8493	98169	838
	2020/04/25	82827	12	4632	77394	8308	98169	801
	2020/04/26	82830	10	4633	77474	8443	98174	723
	2020/04/27	82836	9	4633	77555	8014	98175	648
	2020/04/28	82858	10	4633	77578	8283	98177	647
	2020/04/29	82862	10	4633	77610	8232	98180	619
	2020/04/30	82874	9	4633	77642	7761	98183	599
	2020/05/1	82875	11	4633	77685	7873	98185	557
	2020/05/2	82877	10	4633	77713	7539	98185	531
	2020/05/3	82880	3	4633	77766	7392	98186	481
	2020/05/4	82881	2	4633	77853	7152	98186	395
	2020/05/5	82883	5	4633	77911	6973	98189	339
	2020/05/6	82885	4	4633	77957	6537	98191	295
	2020/05/7	82886	6	4633	77993	6167	98194	260
	2020/05/8	82887	8	4633	78046	5859	98196	208
	2020/05/9	82901	4	4633	78120	5840	98197	148
	2020/05/10	82918	3	4633	78144	5501	98197	141
	2020/05/11	82919	3	4633	78171	5470	98198	115
	2020/05/12	82926	4	4633	78189	5317	98199	104
	2020/05/13	82929	4	4633	78195	5291	98199	101
	2020/05/14	82933	4	4633	78209	5211	98199	91
	2020/05/15	82941	3	4633	78209	5053	98201	89
	2020/05/16	82947	4	4634	78227	4724	98203	86
	2020/05/17	82954	4	4634	78238	4970	98204	82
	2020/05/18	82960	3	4634	78241	5054	98205	85
	2020/05/19	82965	7	4634	78244	4893	98208	87
	2020/05/20	82967	7	4634	78249	4864	98209	84
	2020/05/21	82971	7	4634	78255	4958	98210	82
	2020/05/22	82971	6	4634	78258	5085	98212	79
	2020/05/23	82974	9	4634	78261	5154	98215	79
	2020/05/24	82985	6	4634	78268	5152	98215	83
	2020/05/25	82992	5	4634	78277	5616	98215	81
	2020/05/26	82993	6	4634	78280	5796	98216	79
	2020/05/27	82995	5	4634	78288	5641	98216	73
	2020/05/28	82995	5	4634	78291	5591	98216	70
	2020/05/29	82999	5	4634	78302	5545	98217	63
	2020/05/30	83001	4	4634	78304	5183	98217	63
	2020/05/31	83017	3	4634	78307	4723	98217	76
	2020/06/1	83022	2	4634	78315	4642	98217	73
	2020/06/2	83022	3	4634	78314	4609	98218	73
	2020/06/3	83022	3	4634	78319	4360	98218	69
	2020/06/4	83027	2	4634	78327	4117	98218	66
	2020/06/5	83030	2	4634	78329	3890	98219	67
	2020/06/6	83036	3	4634	78332	3389	98221	70
	2020/06/7	83040	4	4634	78341	3232	98222	65
	2020/06/8	83043	1	4634	78351	2971	98222	58
	2020/06/9	83046	2	4634	78357	2892	98223	55
	2020/06/10	83057	1	4634	78361	3179	98223	62
	2020/06/11	83064	1	4634	78365	3124	98223	65
	2020/06/12	83075	1	4634	78367	3197	98223	74
	2020/06/13	83132	2	4634	78369	3358	98224	129
	2020/06/14	83181	3	4634	78370	3852	98225	177
	2020/06/15	83221	4	4634	78377	4340	98228	210
	2020/06/16	83265	7	4634	78379	4683	98231	252
	2020/06/17	83293	7	4634	78394	5220	98234	265
	2020/06/18	83325	7	4634	78398	5856	98236	293

(*continued on next page*)

Table 2 (*continued*)

Groups	Date	X	P	Z	R	$S_\rho + L\rho$	Y	D
	2020/06/19	83352	11	4634	78410	6023	98240	308
	2020/06/20	83378	13	4634	78413	6339	98243	331
	2020/06/21	83396	15	4634	78413	7236	98245	349
	2020/06/22	83418	15	4634	78425	7591	98247	359
	2020/06/23	83430	18	4634	78428	7557	98251	368
	2020/06/24	83449	13	4634	78433	8011	98251	382
	2020/06/25	83462	10	4634	78439	8044	98254	389
	2020/06/26	83483	8	4634	78444	7876	98251	405
	2020/06/27	83500	8	4634	78451	7445	98252	415
	2020/06/28	83512	10	4634	78460	7012	98256	418
	2020/06/29	83531	7	4634	78469	6809	98257	428
	2020/06/30	83534	8	4634	78479	6479	98259	421
	2020/07/1	83537	5	4634	78487	5910	98259	416
	2020/07/2	83542	6	4634	78499	5589	98260	419
	2020/07/3	83545	7	4634	78509	4993	98262	402
	2020/07/4	83553	7	4634	78516	4201	98263	403
	2020/07/5	83557	7	4634	78518	3988	98263	405
	2020/07/6	83565	7	4634	78528	3940	98265	403
	2020/07/7	83572	6	4634	78548	4214	98265	390
	2020/07/8	83581	5	4634	78590	3840	98265	357
	2020/07/9	83585	8	4634	78609	3796	98268	342
	2020/07/10	83587	8	4634	78623	3580	98268	330
	2020/07/11	83594	7	4634	78634	3739	98268	326
	2020/07/12	83602	7	4634	78648	3494	98268	320
	2020/07/13	83605	5	4634	78674	3267	98268	297
	2020/07/14	83611	3	4634	78693	3577	98268	284
	2020/07/15	83612	3	4634	78719	3313	98268	259
	2020/07/16	83622	3	4634	78737	3651	98269	251
	2020/07/17	83644	4	4634	78758	4072	98270	252
	2020/07/18	83660	4	4634	78775	6925	98271	251
	2020/07/19	83682	4	4634	78799	7204	98272	249
	2020/07/20	83693	1	4634	78817	7108	98272	242
	2020/07/21	83707	1	4634	78840	6988	98272	233
	2020/07/22	83729	4	4634	78855	7218	98275	240
	2020/07/23	83750	2	4634	78873	7526	98276	243
	2020/07/24	83784	2	4634	78889	11500	98278	261
	2020/07/25	83830	3	4634	78908	11762	98280	288
	2020/07/26	83891	3	4634	78918	13935	98280	339
	2020/07/27	83959	1	4634	78934	14590	98280	391
	2020/07/28	84060	1	4634	78944	15034	98280	482
	2020/07/29	84165	2	4634	78957	18353	98281	574
	2020/07/30	84292	2	4634	78974	18461	98282	684
	2020/07/31	84337	2	4634	78989	20278	98282	714
	2020/08/1	84385	2	4634	79003	21445	98282	748
	2020/08/2	84428	4	4634	79013	21585	98285	781
	2020/08/3	84464	5	4634	79030	21743	98286	800
	2020/08/4	84491	3	4634	79047	23018	98286	810
	2020/08/5	84528	2	4634	79057	23985	98286	837
	2020/08/6	84565	3	4634	79088	26499	98288	843
	2020/08/7	84596	7	4634	79123	27357	98293	839
	2020/08/8	84619	6	4634	79168	25822	98293	817
	2020/08/9	84668	7	4634	79232	24055	98294	802
	2020/08/10	84712	3	4634	79284	23790	98296	794
	2020/08/11	84737	3	4634	79342	23039	98297	761
	2020/08/12	84756	4	4634	79398	22498	98298	724
	2020/08/13	84786	5	4634	79462	21456	98300	690
	2020/08/14	84808	3	4634	79519	20441	98301	655
	2020/08/15	84827	3	4634	79575	19933	98302	618
	2020/08/16	84849	4	4634	79630	19907	98304	612
	2020/08/17	84871	3	4634	79642	18473	98304	595
	2020/08/18	84888	2	4634	79685	17093	98304	569
	2020/08/19	84895	2	4634	79745	16369	98304	516
	2020/08/20	84917	0	4634	79792	14599	98304	491
	2020/08/21	84939	1	4634	79851	14305	98305	454
	2020/08/22	84951	3	4634	79895	13730	98307	422
	2020/08/23	84967	2	4634	79925	13220	98308	408
	2020/08/24	84981	2	4634	79961	12370	98308	386
	2020/08/25	84996	0	4634	80015	11915	98308	347
	2020/08/26	85004	1	4634	80046	11227	98309	324
	2020/08/27	85013	3	4634	80091	10040	98311	288
	2020/08/28	85022	0	4634	80126	9148	98311	262
	2020/08/29	85031	0	4634	80153	7787	98311	244
	2020/08/30	85048	0	4634	80177	7190	98311	237
	2020/08/31	85058	0	4634	80208	7546	98311	216
	2020/09/1	85066	0	4634	80234	7587	98311	198

(*continued on next page*)

Table 2 (*continued*)

Groups	Date	X	P	Z	R	$S_\rho + L\rho$	Y	D
	2020/09/2	85077	0	4634	80251	7259	98311	192
	2020/09/3	85102	0	4634	80263	7610	98311	205
	2020/09/4	85112	0	4634	80284	7180	98311	194
	2020/09/5	85122	2	4634	80302	6110	98313	186
	2020/09/6	85134	1	4634	80320	5959	98313	180
	2020/09/7	85144	1	4634	80335	6552	98313	175
	2020/09/8	85146	6	4634	80347	6606	98318	165
	2020/09/9	85153	1	4634	80358	6558	98318	161
	2020/09/10	85168	1	4634	80377	6709	98318	157
	2020/09/11	85174	1	4634	80386	6800	98319	154
	2020/09/12	85184	0	4634	80399	6729	98319	151
	2020/09/13	85194	3	4634	80415	6527	98322	145
	2020/09/14	85202	2	4634	80426	6513	98322	142
	2020/09/15	85214	0	4634	80437	6576	98322	143
	2020/09/16	85223	1	4634	80448	6496	98323	141
	2020/09/17	85255	2	4634	80456	6443	98324	165
	2020/09/18	85269	1	4634	80464	6514	98325	171
	2020/09/19	85279	2	4634	80477	6684	98326	168
	2020/09/20	85291	1	4634	80484	6233	98326	173
	2020/09/21	85297	0	4634	80497	6653	98326	166
	2020/09/22	85307	0	4634	80505	6864	98326	168
	2020/09/23	85314	0	4634	80513	6865	98326	167
	2020/09/24	85322	1	4634	80522	6911	98327	166
	2020/09/25	85337	1	4634	80536	7085	98328	167
	2020/09/26	85351	0	4634	80541	7160	98328	176
	2020/09/27	85372	0	4634	80553	7020	98328	185
	2020/09/28	85384	1	4634	80566	7729	98329	184
	2020/09/29	85403	2	4634	80578	7610	98331	191
	2020/09/30	85414	3	4634	80594	7241	98334	186
	2020/10/1	85424	0	4634	80601	7424	98334	189
	2020/10/2	85434	1	4634	80611	7227	98335	189
	2020/10/3	85450	3	4634	80621	7439	98338	195
	2020/10/4	85470	0	4634	80628	8013	98338	208
	2020/10/5	85482	0	4634	80635	8721	98338	213
	2020/10/6	85489	0	4634	80650	8792	98338	205
	2020/10/7	85500	1	4634	80666	8712	98339	200
	2020/10/8	85521	0	4634	80681	7924	98339	206
	2020/10/9	85536	0	4634	80696	8164	98339	206
	2020/10/10	85557	5	4634	80705	7906	98344	218
	2020/10/11	85578	1	4634	80714	7961	98345	230
	2020/10/12	85591	0	4634	80729	8291	98345	228
	2020/10/13	85611	2	4634	80736	8912	98347	241
	2020/10/14	85622	2	4634	80748	8571	98349	240
	2020/10/15	85646	1	4634	80759	8179	98350	253
	2020/10/16	85659	1	4634	80766	8040	98351	259
	2020/10/17	85672	1	4634	80786	8265	98352	252
	2020/10/18	85685	0	4634	80802	7851	98352	249
	2020/10/19	85704	3	4634	80812	8431	98355	258
	2020/10/20	85715	0	4634	80834	8557	98355	247
	2020/10/21	85729	2	4634	80850	8473	98357	245
	2020/10/22	85747	2	4634	80865	8118	98359	248
	2020/10/23	85775	0	4634	80876	8069	98359	265
	2020/10/24	85790	1	4634	80891	7871	98360	265
	2020/10/25	85810	1	4634	80911	8317	98361	265
	2020/10/26	85826	0	4634	80928	9485	98361	264
	2020/10/27	85868	0	4634	80936	9907	98361	289
	2020/10/28	85915	0	4634	80943	11296	98361	338
	2020/10/29	85940	6	4634	80967	12863	98367	339
	2020/10/30	85973	2	4634	80984	13280	98369	355
	2020/10/31	85997	0	4634	81004	14247	98369	359
	2020/11/1	86021	1	4634	81024	14489	98370	363
	2020/11/2	86070	2	4634	81045	15585	98372	391
	2020/11/3	86087	1	4634	81061	16572	98373	392
	2020/11/4	86115	3	4634	81081	15933	98376	400
	2020/11/5	86151	23	4634	81098	16476	98399	419
	2020/11/6	86184	0	4634	81131	16532	98399	419
	2020/11/7	86212	4	4634	81168	16618	98403	410
	2020/11/8	86245	1	4634	81168	16618	98404	410
	2020/11/9	86267	0	4634	81207	17465	98404	426
	2020/11/10	86284	0	4634	81228	17279	98404	422
	2020/11/11	86299	1	4634	81252	16817	98405	413
	2020/11/12	86307	0	4634	81279	15977	98405	394
	2020/11/13	86325	0	4634	81303	15650	98405	388
	2020/11/14	86338	1	4634	81319	15032	98406	385
	2020/11/15	86346	1	4634	81338	14232	98407	374

(*continued on next page*)

Table 2 (*continued*)

Groups	Date	X	P	Z	R	$S_\rho + L\rho$	Y	D
	2020/11/16	86361	0	4634	81374	13995	98407	353
	2020/11/17	86369	0	4634	81411	13974	98407	324
	2020/11/18	86381	0	4634	81433	13176	98407	314
	2020/11/19	86398	1	4634	81453	12412	98408	311
	2020/11/20	86414	0	4634	81472	11892	98408	308
	2020/11/21	86431	0	4634	81481	11375	98408	316

References

[1] World Health Organization (WHO).https://www.who.int/.
[2] Huang C, Wang Y, Li X, Ren L, Zhao J, Hu Y, Zhang L, Fan G, Xu J, Gu X, Cheng Z, Yu T, Xia J, Wei Y, Wu W, Xie X, Yin W, Li H, Liu M, Xiao Y, Gao H, Guo L, Xie J, Wang G, Jiang R, Gao Z, Jin Q, Wang J, Cao B. Clinical features of patients infected with 2019 novel coronavirus in Wuhan, China. Lancet 2020;395(10223):497–506.
[3] Abdel-Rahman MAM. Academic attitudes toward the role of social media in shaping electronic public opinion about crises an applied study on (corona virus crisis). Inf Sci Lett 2020;9(2):143–60.
[4] Chan JFW, Yuan S, Kok KH, To KKW, Chu H, Yang J, Xing F, Liu J, Yip CCY, Poon RWS, Tsoi HW, Lo SKF, Chan KH, Poon VKM, Chan WM, Ip JD, Cai JP, Cheng VCC, Chen H, Hui CKM, Yuen KY. A familial cluster of pneumonia associated with the 2019 novel coronavirus indicating person-to-person transmission: a study of a family cluster. Lancet 2020;395(10223):514–23.
[5] Killerby ME, Biggs HM, Midgley CM, Gerber SI, Watson JT. Middle east respiratory syndrome coronavirus transmission. Emerg Infect Dis 2020;26(2):191–8.
[6] Li Q, Guan X, Wu P, Wang X, Zhou L, Tong Y, Ren R, Leung KS, Lau EH, Wong JY, Xing X, Xiang N, Wu Y, Li C, Chen Q, Li D, Liu T, Zhao J, Liu M, Tu W, Chen C, Jin L, Yang R, Wang Q, Zhou S, Wang R, Liu H, Luo Y, Liu Y, Shao G, Li H, Tao Z, Yang Y, Deng Z, Liu B, Ma Z, Zhang Y, Shi G, Lam TT, Wu JT, Gao GF, Cowling BJ, Yang B, Leung GM, Feng Z. Early Transmission Dynamics in Wuhan, China, of Novel Coronavirus-Infected Pneumonia. N Engl J Med 2020;382(13):1199–207.
[7] Tang B, Wang X, Li Q, Bragazzi NL, Tang S, Xiao Y, Wu J. Estimation of the Transmission Risk of the 2019-nCoV and Its Implication for Public Health Interventions. J Clin Med 2020;9(2):462.
[8] Alnaser WE, Abdel-Aty M, Al-Ubaydli O. Mathematical Prospective of Coronavirus Infections in Bahrain, Saudi Arabia and Egypt. Inf Sci Lett 2020;9(1):51–64.
[9] Teamah AAM, Afifi WA, Dar Javid Gani, El-Bagoury AH, Al-Aziz SN. Optimal discrete search for a randomly moving COVID19. J Stat Appl Prob 2020;9(3):473–81.
[10] Blackwood JC, Childs LM. An introduction to compartmental modeling for the budding infectious disease modeler. Lett Biomath 2018;5(1):195–221.
[11] Baba IA, Yusuf A, Nisar KS, Abdel-Aty A-H, Nofal TA. Mathematical model to assess the imposition of lockdown during COVID-19 pandemic. Results Phys 2021;20:103716.
[12] Abdulwasaa MA, Abdo MS, Shah K, Nofal TA, Panchal SK, Kawale SV, Abdel-Aty A-H. Fractal-fractional mathematical modeling and forecasting of new cases and deaths of COVID-19 epidemic outbreaks in India. Results Phys 2021;20:103702.
[13] Shahzad M, Abdel-Aty A-H, Attia RAM, Khoshnaw SHA, Aldila D, Ali M, Sultan F. Dynamics models for identifying the key transmission parameters of the COVID-19 disease. Alexand Eng J 2021;60(1):757–65.
[14] Fitzpatrick MC, Bauch CT, Townsend JP, Galvani AP. Modelling microbial infection to address global health challenges. Nat Microbiol 2019;4(10):1612–9.
[15] Zu J, Li M, Li Z, Shen M, Xiao Y, Ji F. Epidemic Trend and Transmission Risk of SARS-CoV-2 after Government Intervention in the Mainland of China: A Mathematical Model Study. SSRN Electron J 2020;9(83):1–14.
[16] Chen TM, Rui J, Wang QP, Zhao ZY, Cui JA, Yin L. A mathematical model for simulating the phase-based transmissibility of a novel coronavirus. Infectious Dis Poverty 2020;9(1):1–8.
[17] Chen T, Rui J, Wang Q, Zhao Z, Cui J-A, Yin L. A Mathematical Model for Simulating the Transmission of Wuhan Novel Coronavirus. bioRxiv (2020) 2020.01.19.911669.
[18] Anastassopoulou C, Russo L, Tsakris A, Siettos C. Data-based analysis, modelling and forecasting of the COVID-19 outbreak. PLOS ONE 2020;15(3):e0230405.
[19] Imai N, Dorigatti I, Cori A, Donnelly C, Riley S, Ferguson NM. Report 2: Estimating the potential total number of novel Coronavirus (2019-nCoV) cases in Wuhan City, China; 2020.https://www.imperial.ac.uk/media/imperial-college/medicine/sph/ide/gida-fellowships/2019-nCoV-outbreak-report-22-01-2020.pdf (accessed Feb 20, 2020).
[20] Zhao S, Lin Q, Ran J, Musa SS, Yang G, Wang W, Lou Y, Gao D, Yang L, He D, Wang MH. Preliminary estimation of the basic reproduction number of novel coronavirus (2019-nCoV) in China, from 2019 to 2020: A data-driven analysis in the early phase of the outbreak. Int J Infectious Dis 92 (2020) 214–217.
[21] Wu JT, Leung K, Leung GM. Nowcasting and forecasting the potential domestic and international spread of the 2019-nCoV outbreak originating in Wuhan, China: a modelling study. Lancet 2020;395(10225):689–97.
[22] Zhao S, Musa SS, Lin Q, Ran J, Yang G, Wang W, Lou Y, Yang L, Gao D, He D, Wang MH. Estimating the Unreported Number of Novel Coronavirus (2019-nCoV) Cases in China in the First Half of January 2020: A Data-Driven Modelling Analysis of the Early Outbreak. J Clin Med 2020;9(2):388.
[23] Sun HG, Zhang Y, Baleanu D, Chen W, Chen YQ. A new collection of real world applications of fractional calculus in science and engineering. Commun Nonlinear Sci Numer Simul 2018;64:213–31.
[24] Baleanu D, Diethelm K, Scalas E, Trujillo JJ. Fractional calculus: Models and numerical methods: 2nd ed., vol. 5, World Scientific Publishing Co., Pte. Ltd.; 2016.
[25] Tarasova VV, Tarasov VE. Concept of dynamic memory in economics. Commun Nonlinear Sci Numer Simul 2018;55:127–45.
[26] Machado JT, Kiryakova V, Mainardi F. Recent history of fractional calculus. Commun Nonlinear Sci Numer Simul 2011;16(3):1140–53.
[27] Giusti A. General fractional calculus and Prabhakar's theory. Commun Nonlinear Sci Numer Simul 2020;83:105114.
[28] Du H, Perré P, Turner I. Modelling fungal growth with fractional transport models. Commun Nonlinear Sci Numer Simul 2020;84:105157.
[29] Yavari M, Nazemi A. On fractional infinite-horizon optimal control problems with a combination of conformable and Caputo-Fabrizio fractional derivatives. ISA Trans 2020;101:78–90.
[30] Khan K, Zarin R, Khan A, Yusuf A, Al-Shomrani M, Ullah A. Stability analysis of five-grade Leishmania epidemic model with harmonic mean-type incidence rate. Adv Difference Eqs 2021;2021(1):1–27.
[31] Kirtphaiboon S, Humphries U, Khan A, Yusuf A. Model of rice blast disease under tropical climate conditions. Chaos Solitons Fractals 2021;143:110530.
[32] Abdon A, Dumitru B. New fractional derivatives with nonlocal and non-singular kernel: Theory and application to heat transfer model. Therm Sci 2016;20:763–9.
[33] Atangana A, Koca I. Chaos in a simple nonlinear system with Atangana-Baleanu derivatives with fractional order. Chaos Solitons Fractals 2016;89:447–54.
[34] Podlubny I. Fractional differential equations: an introduction to fractional derivatives, fractional differential equations, to methods of their solution and some of their applications -. Ghent University Library; 1998.
[35] Singh J, Kumar D, Hammouch Z, Atangana A. A fractional epidemiological model for computer viruses pertaining to a new fractional derivative. Appl Math Comput 2018;316:504–15.
[36] Atangana A. Non validity of index law in fractional calculus: A fractional differential operator with markovian and non-markovian properties. Physica A 2018;505:688–706.
[37] Ameen I, Hidan M, Mostefaoui Z, Ali HM. Fractional Optimal Control with Fish Consumption to Prevent the Risk of Coronary Heart Disease. Complexity 2020;2020:13.
[38] Ali HM, Ameen I. Save the pine forests of wilt disease using a fractional optimal control strategy. Chaos Solitons Fractals 2020;132:109554.
[39] Baleanu D, Jajarmi A, Sajjadi SS, Mozyrska D. A new fractional model and optimal control of a tumor-immune surveillance with non-singular derivative operator. Chaos 2019;29(8):083127.
[40] Kheiri H, Jafari M. Stability analysis of a fractional order model for the HIV/AIDS epidemic in a patchy environment. J Comput Appl Math 2019;346:323–39.
[41] Podlubny I, Tavazoei MS, Vinagre Jara BM, Xue D, Chen YQ, Haeri M. A Special Issue in ISA Transactions "Fractional Order Signals, Systems, and Controls: Theory and Application. ISA Trans 2018;82(1):30527059.
[42] Frunzo L, Garra R, Giusti A, Luongo V. Modeling biological systems with an improved fractional Gompertz law. Commun Nonlinear Sci Numer Simul 2019;74:260–7.
[43] Higazy M. Novel fractional order SIDARTHE mathematical model of COVID-19 pandemic. Chaos Solitons Fractals 2020;138:110007.
[44] Yadav RP. Renu Verma, A numerical simulation of fractional order mathematical modeling of COVID-19 disease in case of Wuhan China. Chaos Solitons Fractals 2020;140:110124.
[45] Tuan NH, Mohammadi H, Rezapour S. A mathematical model for COVID-19 transmission by using the Caputo fractional derivative. Chaos Solitons Fractals 2020;140:110107.
[46] Shaikh AS, Shaikh IN, Nisar KS. A mathematical model of COVID-19 using fractional derivative: outbreak in India with dynamics of transmission and control. Adv Difference Eqs 2020;2020(1):373.
[47] Khan MA, Atangana A. Modeling the dynamics of novel coronavirus (2019-nCov) with fractional derivative. Alexand Eng J 2020;59(4):2379–89.
[48] Khan MA, Atangana A, Alzahrani E. Fatmawati, The dynamics of covid-19 with quarantined and isolation. Adv Difference Eqs 2020;2020(1):1–22.
[49] Atangana E, Atangana A. Facemasks simple but powerful weapons to protect against covid-19 spread: Can they have sides effects. Results Phys 2020;19:103425.
[50] Atangana A. Modelling the spread of covid-19 with new fractal-fractional operators: Can the lockdown save mankind before vaccination. Chaos Solitons Fractals 2020;136:109860.
[51] Khoshnaw SH, Salih RH, Sulaimany S. Mathematical modelling for coronavirus disease (COVID-19) in predicting future behaviours and sensitivity analysis. Math Modell Natural Phenomena 2020;15:33.

[52] Atangana A, Araz SI. Modeling and forecasting the spread of COVID-19 with stochastic and deterministic approaches: Africa and Europe. Adv Difference Eqs 2021;2021(1):1–107.
[53] Safare KM, Betageri VS, Prakasha DG, Veeresha P, Kumar S. A mathematical analysis of ongoing outbreak COVID-19 in India through nonsingular derivative. Numer Methods Partial Differential Eqs 2021;37(2):1282–98.
[54] Kumar S, Chauhan RP, Momani S, Hadid S. Numerical investigations on COVID-19 model through singular and non singular fractional operators. Numer Methods Partial Differential Eqs 2020;2020:1–27.
[55] Atangana E, Atangana A. Facemasks simple but powerful weapons to protect against COVID-19 spread: Can they have sides effects? Results Phys 2020;19:103425.
[56] Atangana EA, Atangana A. NC-ND license Facemasks simple but powerful weapons to protect against COVID-19 spread: Can they have sides effects? Results Phys 2020;10:103425.
[57] Ahmed I, Baba IA, Yusuf A, Kumam P, Kumam W. Analysis of Caputo fractional-order model for COVID-19 with lockdown. Adv Difference Eqs 2020;2020(1):1–14.
[58] Backer JA, Klinkenberg D, Wallinga J. Incubation period of 2019 novel coronavirus (2019-nCoV) infections among travellers from Wuhan, China, 20–28 January 2020. Eurosurveillance 2020;25(5):2000062.
[59] Lauer SA, Grantz KH, Bi Q, Jones FK, Zheng Q, Meredith H, Azman AS, Reich NG, Lessler J. The incubation period of 2019-nCoV from publicly reported confirmed cases: estimation and application, Ann Internal Med (2020) 2020.02.02.20020016.
[60] Van Den Driessche P, Watmough J. Reproduction numbers and sub-threshold endemic equilibria for compartmental models of disease transmission. Math Biosci 2002;180(1–2):29–48.
[61] Commault C. Mathematical systems theory (third edition), G.J. Olsder and J.W. van der Woude, VSSD, Delft, The Netherlands, 2005, 208pp., ISBN 90-71301-40-0, Int J Robust Nonlinear Control 16(2) (2006) 87–88.
[62] Diethelm K, Ford NJ, Freed AD. Detailed error analysis for a fractional Adams method. Numer Algorithms 2004;36(1):31–52.
[63] Garrappa R. On linear stability of predictor–corrector algorithms for fractional differential equations. Int J Comput Math 2010;87(10):2281–90.
[64] Ameen I, Novati P. The solution of fractional order epidemic model by implicit Adams methods. Appl Math Model 2017;43:78–84.